

A Comparison of the PSCz and Stromlo-APM Redshift Surveys

M.D. Seaborne¹, W. Sutherland¹, H. Tadros¹, G. Efstathiou², C.S. Frenk³,
O. Keeble⁴, S. Maddox², R.G. McMahon², S. Oliver⁴, M. Rowan-Robinson⁴,
W. Saunders⁵, S.D.M. White⁶

¹ Dept. of Physics, Keble Road, Oxford OX1 3RH, UK

² Institute of Astronomy, Madingley Road, Cambridge CB3 0HA, UK

³ Dept. of Physics, South Road, Durham DH1 3LE, UK

⁴ Astrophysics Group, Imperial College, Blackett Laboratory, Prince Consort Road, London SW7 2BZ, UK

⁵ Royal Observatory, Blackford Hill, Edinburgh, EH9 3HJ, UK

⁶ Max Planck Institute for Astrophysik, Karl-Schwarzschild-Strasse 1, D-8046 Garching bei Munchen, Germany.

WJS, 20 Jan 98.

ABSTRACT

We present a direct comparison of the clustering properties of two redshift surveys covering a common volume of space: the recently completed *IRAS* Point Source Catalogue redshift survey (PSCz) containing 14500 galaxies with a limiting flux of 0.6 Jy at 60 μm , and the optical Stromlo-APM survey containing 1787 galaxies in a region of 4300 deg^2 in the south Galactic cap. We use three methods to compare the clustering properties: the counts-in-cells comparison of Efstathiou (1995, hereafter E95), the two-point cross correlation function, and the Tegmark (1998) ‘null-buster’ test. We find that the Stromlo variances are systematically higher than those of PSCz, as expected due to the deficit of early-type galaxies in *IRAS* samples. However we find that the differences between the cell counts are consistent with a linear bias between the two surveys, with a relative bias parameter $b_{\text{rel}} \equiv b_{\text{Stromlo}}/b_{\text{PSCz}} \approx 1.3$ which appears approximately scale-independent. The correlation coefficient R between optical and *IRAS* densities on scales $\sim 20 h^{-1}\text{Mpc}$ is $R \geq 0.72$ at 95% c.l., placing limits on types of ‘stochastic bias’ which affect optical and *IRAS* galaxies differently.

Key words: surveys – galaxies:clusters:general – large-scale structure of Universe

1 INTRODUCTION

Observations of galaxy clustering are a very valuable probe of cosmology, since they can provide information both on the shape of the initial density fluctuations and on the cosmological parameters such as Ω_0 , the composition of the dark matter etc. When combined with related observables such as CMB anisotropy and galaxy peculiar motions, it should in future be possible to perform consistency checks since there are 3 observable functions (the CMB spherical harmonics and the power spectra of density and velocity fields) predicted by one input function (the initial power spectrum) and a handful of cosmological parameters.

Following the pioneering studies by Peebles and coworkers in the 1970s, the field has undergone rapid growth, with many large galaxy surveys now in exist-

tence, notably the 2-dimensional APM Galaxy Survey (Maddox *et al.* 1990), the CfA-2 redshift survey (e.g. Vogeley *et al.* 1992), the Las Campanas redshift survey (Shectman *et al.* 1996) and the *IRAS* PSCz survey (Saunders *et al.* 1997).

The galaxy surveys obviously measure the distribution of luminous matter, which probably does not exactly trace the total mass distribution which is dominated by dark matter. For instance, it was shown by Kaiser (1984) that if galaxies form at peaks of a Gaussian random field, they will be more strongly clustered than the underlying mass, dubbed biasing. Thus, understanding the relationship between galaxies and mass is important both for estimation of cosmological parameters and for probing the physics of galaxy formation. A common assumption is ‘linear biasing’ given by $\delta_g = b\delta_m$ where δ_g, δ_m are the fractional overdensities

relative to the mean in galaxies and mass respectively, and b is a constant ‘bias parameter’; this assumption must be inaccurate on small scales for $b > 1$ since $\delta_g \geq -1$. However, we may still define a bias parameter $b(r)$ by e.g. $\xi_{gg}(r) = b(r)^2 \xi_{mm}(r)$, and if the biasing is ‘local’ in the sense that the galaxy density is a function only of the mass density smoothed on small scales, it can be shown that $b(r)$ must approach a constant on large scales (e.g. Coles 1993, Pen 1998). A detailed account of the statistics of biasing including possible non-linearities and stochastic variations, and the relationships between the several possible definitions of b , is given by Dekel & Lahav (1998). Recently, there have been a number of predictions of bias assuming that galaxies correspond to dark matter halos, e.g. the analytic model of Mo & White (1996), which is compared with N-body simulations by e.g. Jing (1998) and Kravtsov & Klypin (1998). The bias factor assuming various simple prescriptions for the morphology-density relation is investigated by Narayanan *et al.* (1998).

Surveys of galaxy peculiar motions can directly map the mass distribution in the local universe, but the error bars per galaxy are large and so the method is limited to rather local volumes with heavy smoothing. Since it is difficult to measure the mass distribution directly, another useful probe is to compare the clustering properties of galaxy surveys with different selection criteria: if these cluster differently, at least one class cannot exactly follow the mass distribution. However, if both classes obey the linear bias relation with different values of b , there is clearly a linear relation between the two galaxy density fields and thus the cross correlation function $\xi_{12}(r) = \sqrt{\xi_1(r)\xi_2(r)}$ where ξ_1, ξ_2 are the usual autocorrelation functions for the two galaxy classes. Thus, if this relation does not hold, then the linear-bias model must fail for at least one of the galaxy classes.

It is well known (e.g. Dressler 1980; Guzzo *et al.* 1997) that the fraction of elliptical galaxies increases with local galaxy density, and it is also known that *IRAS* galaxies (selected at $60\mu\text{m}$) have a lower correlation amplitude on small scales than optically selected galaxies (e.g. Saunders *et al.* 1992; Loveday *et al.* 1995). It is also known that the density fields of optical and *IRAS* galaxies are in quite good qualitative agreement, i.e. the prominent nearby structures such as Virgo, Perseus-Pisces, Hydra-Centaurus are common to both types of survey, but quantitative comparisons so far have been rather limited in volume since the differing depths and sky coverages cause limited overlap between the different surveys (e.g. Oliver *et al.* 1996). Probably for this reason, there has been considerable scatter in previous estimates of the relative bias b_O/b_I (e.g. Lahav, Nemiroff & Piran 1992). A comparison of *velocity* fields predicted from *IRAS* 1.2 Jy and ORS surveys is given by Baker *et al.* (1998), who find very good agreement between the two velocity fields for a relative bias factor $b_{\text{rel}} = b_O/b_I \approx 1.4$. In this paper we provide a compari-

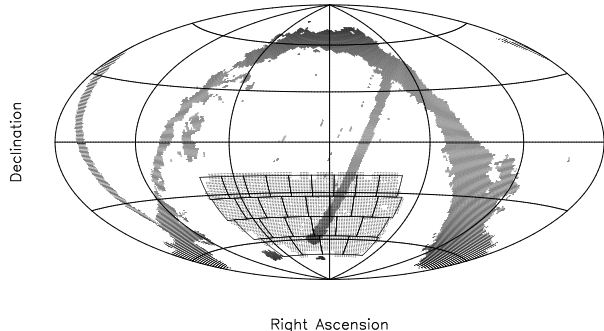


Figure 1: An Aitoff projection of the PSCz and Stromlo-APM regions in equatorial coordinates. The PSCz mask is indicated by the dark shading. The light shaded area in the southern hemisphere is the Stromlo survey region. An example of one of the shells of cells is also shown.

son of density fields over a larger volume of space than previously available, using the newly-completed *IRAS* PSCz redshift survey and the sparse-sampled Stromlo-APM optical survey.

The plan of the paper is as follows: we summarise details of the two surveys in §2, and then compare the clustering with three different statistical methods: a counts-in-cells comparison in §3, two-point correlation functions in §4 and the ‘modified χ^2 ’ statistic of Tegmark (1998) in §5. We summarise the conclusions in §6.

2 THE PSCZ AND STROMLO-APM REDSHIFT SURVEYS

The PSCz survey is described in detail by Saunders *et al.* (1997). The aim of the survey was to obtain redshifts for all *IRAS* galaxies with $60\mu\text{m}$ fluxes greater than 0.6 Jy over as much of the sky as possible. The parent catalogue is based on the QMW *IRAS* Galaxy Catalogue (Rowan-Robinson *et al.* 1990) but with a number of modifications designed to increase sky coverage and improve completeness. The final 2-D catalogue contains 17060 objects, 1593 of which were rejected as sources in our Galaxy or multiple entries from resolved nearby galaxies. Another 648 were rejected as faint galaxies or no optical identification leaving 14819 in the target list. Redshifts are now known for 14539 (95%) of these. The PSCz mask is shown in figure 1 as the dark shaded region. It includes regions of low galactic latitude, some odd patches of galactic cirrus and the two strips of ecliptic longitude not surveyed by *IRAS*.

The Stromlo-APM survey (Loveday *et al.* 1992)

is an optically selected redshift survey in a region of the southern hemisphere approximately $21^{\text{h}} \lesssim \alpha \lesssim 5^{\text{h}}$, $-72.5^{\circ} \lesssim \delta \lesssim -17.5^{\circ}$. The survey consists of 1787 galaxies of magnitude $b_j \leq 17.15$ selected at a rate of 1 in 20 from the APM galaxy catalogue. The Stromlo-APM region is shown by the light shading in figure 1. The small holes in the survey are mainly due to bright foreground stars. Figure 2 shows ‘cone plots’ of galaxies in declination slices for the two catalogues in the APM region. Note that the selection functions are somewhat different, with dN/dz peaking at $\sim 70 h^{-1}\text{Mpc}$ for PSCz and $\sim 150 h^{-1}\text{Mpc}$ for Stromlo, and the shot noise is appreciable in both surveys due to the relatively low space density of *IRAS* galaxies and the 1-in-20 sampling for Stromlo. However, there is quite good qualitative similarity between the two distributions, e.g. the prominent ‘wall’ near $\alpha \sim 21^{\text{h}}$ and the squarish void centred on $\delta \sim -40^{\circ}$, $cz \sim 7000 \text{ km s}^{-1}$.

In the following analysis we treat the two galaxy surveys as independent samples of the same region of the universe. This assumption would not be valid if there were an appreciable number of galaxies common to both catalogues. We have found 41 such galaxies and these have not been included in any of the subsequent analysis.

2.1 Mock PSCz and Stromlo-APM catalogues

Throughout this paper we used a suite of mock PSCz and Stromlo-APM surveys to estimate the uncertainty in the various statistics calculated. There are 27 pairs of mock catalogues in total taken from N-body simulations of standard $\Omega_0 = 1$ CDM universes. They have the same survey geometry, selection function and sampling rate as their real counterparts. Each pair of Stromlo and PSCz catalogues was sampled from a common region of space in the same initial simulation so that underlying density fluctuations in the PSCz mock catalogue are mirrored in the corresponding Stromlo catalogue. We would therefore expect to see the clustering in each catalogue of the pair to differ only due to the shot noise. This property is useful when calculating the uncertainty in the cross correlation function and the ratio between the two individual correlation functions. Mass points in the simulations are interpreted as galaxies so the catalogues do not include bias.

3 COUNTS IN CELLS COMPARISON

The counts in cells comparison method is discussed in detail in E95. The surveyed region of space is divided into spherical shells of thickness ℓ centred on the observer. Each shell is then subdivided into N_c approximately cubic cells each of volume $V = \ell^3$. For one catalogue, we represent the galaxy counts in the i th cell by N_i . The expected mean cell count is denoted by

$\langle N_i \rangle = \lambda$. The variance of the counts in cells in excess of Poisson variance is given by

$$S_1 = \frac{1}{N_c - 1} \sum_i (N_i - \bar{N})^2 - \bar{N}. \quad (1)$$

where \bar{N} is the mean cell count. The expectation value of (1) is

$$\langle S_1 \rangle = \lambda^2 \sigma_1^2, \quad (2)$$

where σ_1^2 is the variance of the underlying density field on the scale of ℓ^3 . This is equal to a volume integral of the autocorrelation function, $\xi(r_{12})$, over the cell of size ℓ^3

$$\sigma_1^2 = \frac{1}{V^2} \iint_{V=\ell^3} \xi(r_{12}) dV_1 dV_2. \quad (3)$$

When the underlying density fluctuations are Gaussian the variance of S_1 is given by

$$\text{Var}(S_1) = \frac{1}{N_c} [2\lambda^2(1 + \sigma_1^2) + 4\lambda^3\sigma_1^2 + 2\lambda^4\sigma_1^4]. \quad (4)$$

The statistics S_1 and S_2 can be found for the two redshift surveys (the subscripts now refer to the two individual surveys) and used to examine the comparative clustering. If the two surveys occupy a common region of space then the comparison can be taken a stage further by computing the covariance, S_{12} , of the cell counts:

$$S_{12} = \frac{1}{(N_c - 1)} \sum_i (N_i - \bar{N})(M_i - \bar{M}) \quad (5)$$

where N_i and M_i now represent the counts from surveys 1 and 2 respectively. The underlying covariance σ_{12}^2 is defined equivalently to σ_1^2 so that

$$\begin{aligned} \langle S_{12} \rangle &= \lambda \mu \sigma_{12}^2, \text{ where} \\ \sigma_{12}^2 &= \frac{1}{V^2} \iint_{V=\ell^3} \xi_{12}(r_{12}) dV_1 dV_2 \end{aligned} \quad (6)$$

where $\mu = \langle M_i \rangle$, the expected cell mean cell count from survey two, and $\xi_{12}(r)$ is the usual two-point cross-correlation function.

To calculate the uncertainty in the statistics S_1 , S_2 and S_{12} we must first assume a model (e.g. Gaussian) for the clustering. The need for such a model can be avoided if we consider only the *differences* between the counts from surveys 1 and 2 in each cell. The normalised mean square difference between the cell counts is

$$S_d = \frac{1}{(N_c - 1)} \sum_i (\bar{M}N_i - M_i\bar{N})^2 - (\bar{M} + \bar{N})\bar{M}\bar{N}. \quad (7)$$

If the galaxy distributions in the two catalogues are Poisson point processes with identical statistical properties then the statistic S_d will be solely determined by Poisson statistics and its variance will be given by

$$\text{Var}(S_d) \approx \lambda \mu \frac{N_c}{(N_c - 1)^2} [\lambda^3 + \mu^3 + 4\lambda^2\mu^2 + 2(\lambda^3\mu + \lambda\mu^3)]. \quad (8)$$

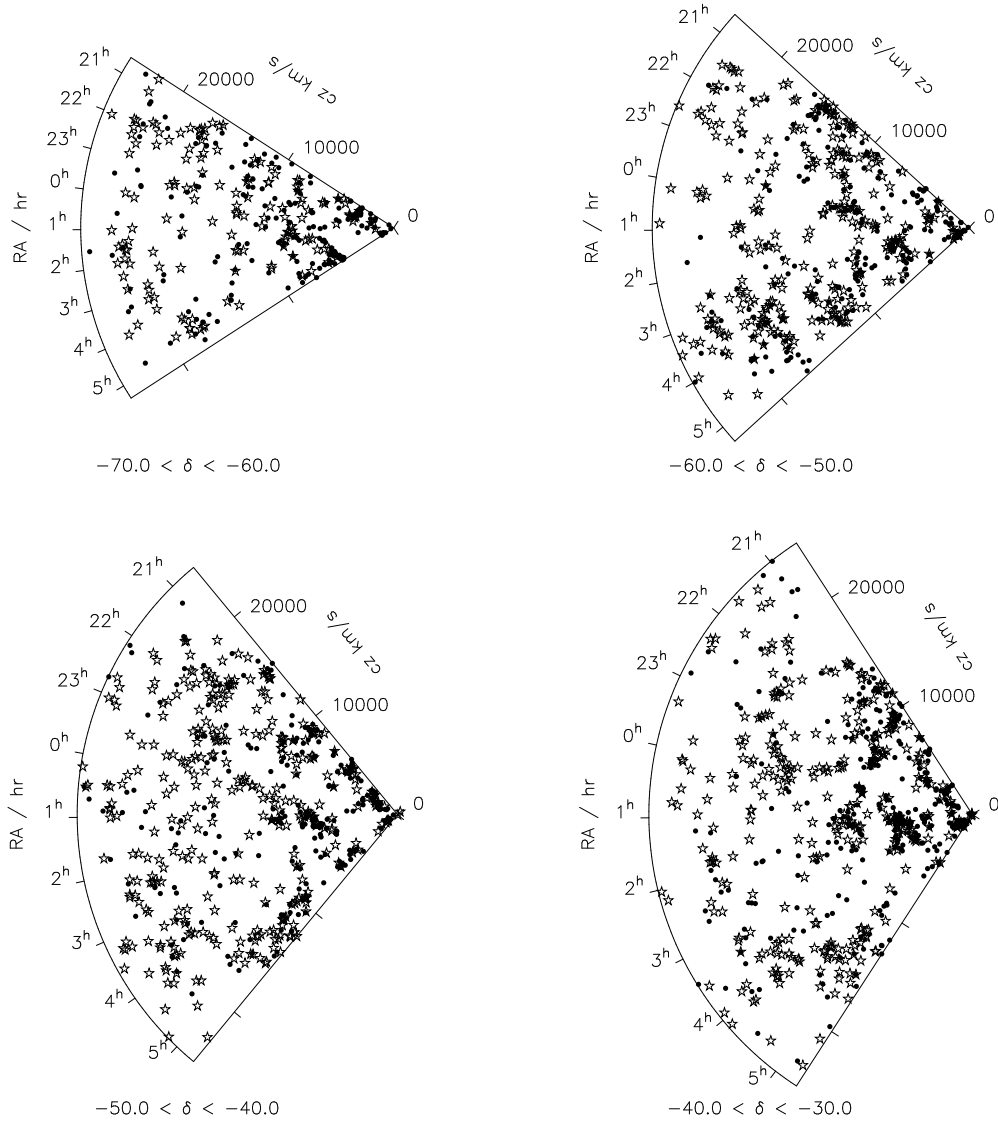


Figure 2: The locations of galaxies in redshift space at slices of declination within the APM region. PSCz galaxies are represented by black spots and Stromlo-APM galaxies by stars.

This value is independent of the underlying nature of the galaxy density field. The statistic S_d is related to S_1 , S_2 and S_{12} by

$$S_d = \bar{M}^2 S_1 + \bar{N}^2 S_2 - 2\bar{M}\bar{N}S_{12} \quad (9)$$

and its expectation value is therefore

$$\langle S_d \rangle = \lambda^2 \mu^2 (\sigma_1^2 + \sigma_2^2 - 2\sigma_{12}^2). \quad (10)$$

This provides an simple way of determining whether the clustering properties of the two surveys are consistent while avoiding making any special assumptions about the nature of the clustering. If the two catalogues sample the same density field then the three correlation functions ξ_1 , ξ_2 and ξ_{12} will be identical and we see from equations (3) and (7) that so too are σ_1^2 , σ_2^2 and σ_{12}^2 . The expectation value of S_d given in equation (10) would therefore be zero within the limits of the sampling error given by equation (8).

We also investigate the possibility that the galaxies in the two catalogues are biased tracers of the same underlying density field. In particular we look at the linear bias model $(\delta\rho/\rho)_{\text{gal}} = b(\delta\rho/\rho)_m$ where the two overdensity fields are perfectly correlated. If b_1 and b_2 are the bias parameters of the two catalogues with respect to the underlying matter distribution then the linear bias model implies

$$\begin{aligned} \sigma_1^2 &= b_1^2 \sigma_m^2, \\ \sigma_2^2 &= b_2^2 \sigma_m^2, \\ \sigma_{12}^2 &= b_1 b_2 \sigma_m^2. \end{aligned} \quad (11)$$

where σ_m^2 is the variance of the underlying density field. Hence we can estimate the relative bias b_1/b_2 . The above clearly implies

$$\sigma_{12}^2 = \sigma_1 \sigma_2 \quad (12)$$

which can be used to test for consistency with linear bias.

The above equations for the S_i 's apply to a single spherical shell with constant mean densities λ, μ . For the full surveys, we now consider a series of N_{shell} spherical shells, each of thickness ℓ , centred on the observer, subdivided into cubical cells as before. The statistics S_1^k , S_2^k and S_d^k are now computed separately for each shell k .

When the number of cells, N_c , is large, the central limit theorem states that the probability distribution of the S_1^k , S_2^k and S_d^k will tend to a multivariate Gaussian

$$p(S_1^k, S_2^k, S_d^k) dS_1^k dS_2^k dS_d^k = \frac{\exp(A) dS_1^k dS_2^k dS_d^k}{(2\pi)^{3/2} (\det \mathbf{V})^{1/2}}, \quad (13)$$

where

$$A = -\frac{1}{2} \sum_{i,j} (S_i - \langle S_i \rangle)(S_j - \langle S_j \rangle)(V^{-1})_{ij}, \quad (14)$$

and V_{ij} is the covariance matrix $V_{ij} = \text{Cov}(S_i^k, S_j^k)$ ($i, j = 1, 2, d$). Expressions for the el-

ements of this matrix can be found in the appendix of E95. We form the combined likelihood over all shells,

$$\mathcal{L} \propto \prod_{k=1}^{N_{\text{shell}}} p(S_1^k, S_2^k, S_d^k) \quad (15)$$

which we maximise with respect to σ_1^2 , σ_2^2 and σ_{12}^2 . This method automatically assigns a weight to each shell. Nearby shells contribute little weight because the number of cells is small and distant shells contribute little information because the statistics become dominated by shot noise.

We use lines of constant right ascension and declination as the cell boundaries to match the geometry of the Stromlo-APM survey region. An example of one of the concentric shells of cells is shown in figure 1. Each cell at right ascension α and declination δ subtends an angle $\Delta\delta$ in declination and has a right ascension range $\Delta\alpha$ such that $\Delta\alpha = \Delta\delta / \cos \delta$. The angle $\Delta\delta$ is chosen at each radial distance to ensure that the sides of the cell are of length ℓ , the shell separation.

We apply a joint PSCz-Stromlo mask to both surveys so that Stromlo galaxies within the PSCz mask are not included and vice versa. A number of the cells are partially or totally covered by the mask. We correct for this by replacing equation (1) with the expression

$$S_i^2 = A/B \quad \text{where} \quad (16)$$

$$\begin{aligned} A &= \left(\frac{V}{N_c} \sum_j \frac{N_j}{V_j} \right)^2 \left\{ \sum_j \left(N_j - V_j \frac{\sum_k N_k}{\sum_k V_k} \right)^2 \right. \\ &\quad \left. - \left[1 - \frac{\sum_k V_k^2}{(\sum_k V_k)^2} \right] \sum_j N_j \right\}, \\ B &= \left(\frac{\sum_j N_j}{\sum_j V_j} \right)^2 \times \\ &\quad \left[\sum_k V_k^2 - 2 \frac{\sum_k V_k^3}{\sum_k V_k} + \frac{(\sum_k V_k^2)^2}{(\sum_k V_k)^2} \right] \end{aligned}$$

(Efstathiou et al. (1990)) where the sum extends over all cells in the i^{th} radial shell and V_j is the volume of cell j not excluded by the mask. This expression is only valid when a small fraction of each cell is excluded by the mask. Cells that are greater than 30% covered by the joint mask were therefore not used in the analysis. To calculate the statistic S_d and the mean cell counts \bar{N} and \bar{M} we artificially increase the galaxy counts in partially filled cells to account for the fraction excluded by the mask.

If we wish to use equation (13) to calculate the likelihood then there must be enough cells in a given radial shell for the central limit theorem to be applicable. Any shells that do not contain enough cells for this to be the case must be excluded from the analysis. We have only included shells with 20 or more filled ($\leq 30\%$ masked) cells. The nearest shells are therefore rejected. Cells be-

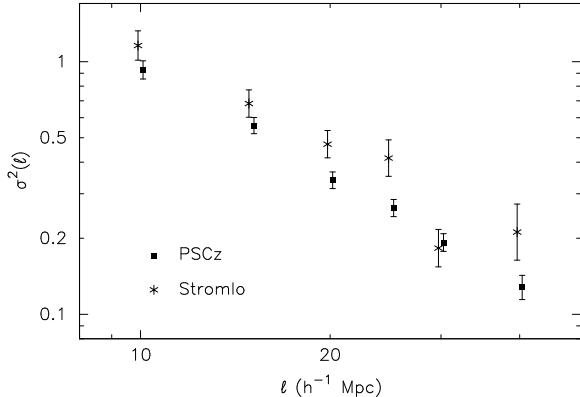


Figure 3: σ^2 as a function of cell size ℓ for the PSCz and Stromlo surveys. The error bars are 1 standard deviation.

yond a radial distance of $250 h^{-1}\text{Mpc}$ are not included in the analysis as they contain very few galaxies and so make a negligible contribution to the final result. The PSCz survey is only complete out to this distance for $|b| \geq 10^\circ$. We therefore mask this region from the PSCz (this has no effect on the ‘combined’ mask since the Stromlo survey is at $b \lesssim -40^\circ$).

Before doing the cell by cell comparison described above we first measure the values of the cell count variances calculated using the whole of each survey; these are shown as a function of cell size in Figure 3. We attempt to minimise the loss of information that arises from binning the data into cells by shifting the entire grid of cells and recalculating the likelihood. We shift the grid by either 0 or $\ell/2$ from the ‘default’ value in combinations of right ascension, declination and radial velocity, thus giving eight separate (although not statistically independent) estimates of the likelihood.

For each of the 8 grid positions we form the individual one dimensional likelihood

$$\mathcal{L}(\sigma_1^2) = \prod_{k=1}^{N_{\text{shell}}} \frac{1}{2\pi\text{Var}(S_1^i)} \exp\left[-\frac{(S_1^i - \bar{N}^2\sigma_1^2)^2}{2\text{Var}(S_1^i)}\right] \quad (17)$$

We obtain the final estimates of σ_1^2, σ_2^2 by computing the product of the eight likelihood functions and finding the maximum; this should provide a better estimate of the peak than using a single grid position alone. However, it is not possible to use the combined likelihood to estimate the uncertainty in the values as the results from each grid position are not independent. We generate the error bars in Figure 3 by repeating the analysis on the 27 mock PSCz and Stromlo catalogues, and measuring the standard deviation of the σ^2 values estimated as above. From the simulations, combining the results from the eight grid positions gives a 20-40% gain in precision in the values of $\log \sigma^2$ over the use of a single set of cells.

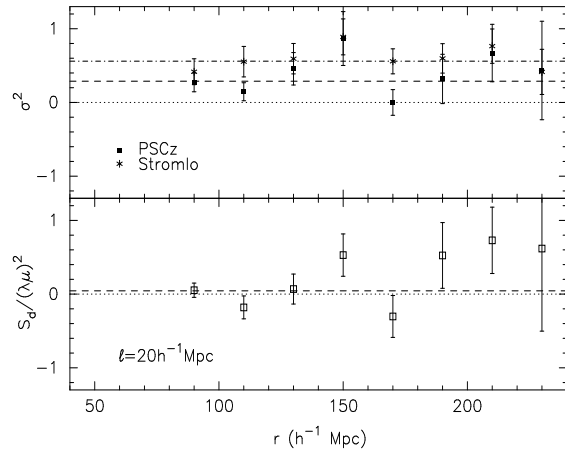


Figure 4: A comparison of the counts in $20 h^{-1}\text{Mpc}$ cells for PSCz and Stromlo galaxies. The top panel shows the values of σ^2 for the two catalogues as a function of radial distance. These are obtained directly from the statistics S_1 and S_2 . The dashed lines show the respective maximum likelihood values calculated with the assumption $\sigma_{12}^2 = \sigma_1\sigma_2$. The lower panel shows the statistic S_d . The maximum likelihood value is calculated with the same assumption and using equation 10. All error bars show one standard deviation.

The gain in precision in general increases with cell size. The observed sum of the eight $\log \mathcal{L}$'s is then re-scaled so that the standard deviation of $\log \sigma^2$ matches that from the simulations.

As expected, the variances decrease with increasing cell size as the galaxy distribution approaches homogeneity on larger scales, and the Stromlo variances are consistently higher than those of PSCz. For cells of sizes 20, 25 and $40 h^{-1}\text{Mpc}$ the error bars do not overlap suggesting that the differences in clustering amplitude are highly significant. Only at $30 h^{-1}\text{Mpc}$ are the values comparable.

Figure 4 shows the values of σ_1^2, σ_2^2 and the statistic S_d for each radial shell, for a cell size of $20 h^{-1}\text{Mpc}$, using Stromlo and PSCz galaxies within the APM region only.

Again we see that the Stromlo variances are, in general, higher. The maximum likelihood value of the statistic S_d lies slightly above zero and has a reduced χ^2 of 1.3 (when compared to the value zero) suggesting a slight difference in the clustering of galaxies in the two catalogues.

3.1 Linear bias

We next consider whether these clustering differences are in agreement with a linear relative bias $\sigma_{\text{optical}} = b_{\text{rel}}\sigma_{\text{IRAS}}$. The likelihood function (equation (15)) is a function of the three parameters σ_1^2, σ_2^2 and σ_{12}^2 ; it is

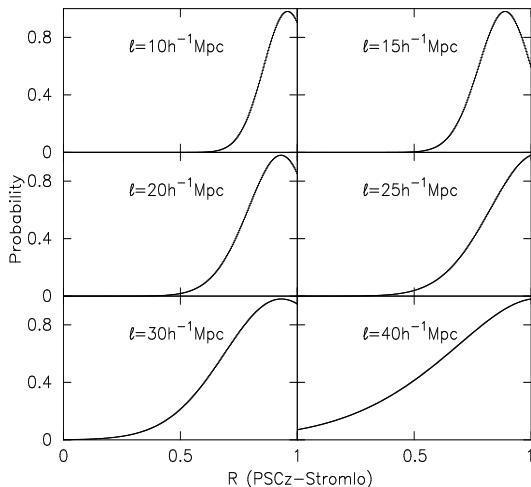


Figure 5: The likelihood as a function of the correlation coefficient R .

more convenient to change the third parameter to the correlation coefficient $R = \sigma_{12}^2 / \sigma_1 \sigma_2$, since we must have $-1 \leq R \leq 1$ in order that the covariance matrix in eq. 13 is positive definite. Linear bias clearly implies $R = 1$. We then assume a uniform prior in the space of $(\log \sigma_1^2, \log \sigma_2^2, R)$ and then integrate \mathcal{L} over the $\log \sigma^2$'s to obtain a one-dimensional likelihood function for R ; this is shown in Figure 5 for cell sizes in the range $10 - 40 h^{-1} \text{Mpc}$. Again, each value of the likelihood $\mathcal{L}(R)$ was calculated using eight different cell grid positions, and the values given are the geometric mean of these eight values. No attempt has been made to reduce the width of the curves to account for the gain in precision obtained from the use of multiple grid positions.

For cells of size 25 and $40 h^{-1} \text{Mpc}$ the maximum likelihood value of R occurs at $R = 1$, consistent with linear bias. Values of R greater than unity are of course unphysical since this would imply that the correlation between the galaxy counts is better than perfect. However, it is not unreasonable for the derivative of the likelihood function to be positive at $R = 1$, if the Poisson differences in the real cell counts happens to be smaller than the ‘ensemble average’ value. For cells of size 10, 15, 20 and $40 h^{-1} \text{Mpc}$ we find that $R_{\text{max}} = 0.96, 0.89, 0.93$ and 0.93 respectively, though in each case $R = 1$ is well within one standard deviation of this. We conclude that the galaxy cell counts are consistent with a linear bias model, and we derive 95% confidence lower limits of $R \geq 0.83, 0.72, 0.55$ for cells of size 10, 20, $30 h^{-1} \text{Mpc}$ respectively.

Figure 6 shows contour maps of the joint likelihood assuming a linear bias, $\mathcal{L}(\sigma_1^2, \sigma_2^2, R = 1)$, for cells of size $10 - 40 h^{-1} \text{Mpc}$. Again we repeat the analysis using the eight different grid positions, and compute the geometric mean of the individual \mathcal{L} 's. This improves our estimate of the peak location but the contours do not

then accurately reflect our improved knowledge of the two variances. Thus, we compute the value of σ^2 for the 27 pairs of mock catalogues, this time using only galaxies that lie outside the joint mask. We finally rescale the mean $\log \mathcal{L}$ so the width of the function matches that in the simulations.

We approximate the shape of the likelihood function to that produced by two Gaussian distributions such that the value of $2 \ln(\mathcal{L}/\mathcal{L}_{\text{max}})$ has a chi-squared distribution with two degrees of freedom. This approximation was tested by directly determining the value of the contour that contains 95% of the likelihood enclosed within a large area of the $\sigma_1^2 - \sigma_2^2$ ($R = 1$) plane. For each cell size examined the 95% contour (shown in bold in figure 6) accurately coincided with the contour $2 \ln(\mathcal{L}/\mathcal{L}_{\text{max}}) = 5.99$ which is the 5th percentile point of the χ^2 distribution with two degrees of freedom.

For cells of size $15 - 30 h^{-1} \text{Mpc}$ we rule out the hypothesis of equal bias as the line $\sigma_1^2 = \sigma_2^2$ lies well outside the 95% confidence interval. The variance of the counts in cells for Stromlo-APM are clearly larger than those for PSCz. For cells of size 10 and $40 h^{-1} \text{Mpc}$ a unit bias is marginally consistent with the larger errors, but a value > 1 is still favoured. All the cell sizes are consistent with a scale-independent relative bias of $b_{\text{rel}} = b_{\text{Stromlo}}/b_{\text{PSCz}} \approx 1.4$.

Table 1 shows the relative bias for each cell size. The value b_{rel}^2 is given by the ratio of the maximum likelihood variances $\sigma_{\text{Stromlo}}^2 / \sigma_{\text{PSCz}}^2$. The 95% confidence interval was found by determining the two straight lines $\sigma_{\text{Stromlo}}^2 = b_{\text{min}}^2 \sigma_{\text{PSCz}}^2$ and $\sigma_{\text{Stromlo}}^2 = b_{\text{max}}^2 \sigma_{\text{PSCz}}^2$ on the contour plots between which 95% of the total likelihood lies.

4 THE TWO-POINT AND CROSS-CORRELATION FUNCTIONS

The linear bias model predicts that the individual two-point correlation functions, ξ_1 and ξ_2 , will be related to the cross-correlation function, ξ_{12} , by

$$\xi_{12} = (\xi_1 \xi_2)^{1/2}. \quad (18)$$

The three correlation functions were found for the galaxies within the common survey region using the estimators

$$\begin{aligned} \xi_1(r) &= \frac{\langle D_1 D_1 \rangle \langle R_1 R_1 \rangle}{\langle D_1 R_1 \rangle^2} - 1 \\ \xi_{12}(r) &= \frac{\langle D_1 D_2 \rangle \langle R_1 R_2 \rangle}{\langle D_1 R_2 \rangle \langle D_2 R_1 \rangle} - 1 \end{aligned} \quad (19)$$

(Hamilton 1993) where the notation $\langle DD \rangle$, $\langle RR \rangle$ and $\langle DR \rangle$ refers to the (weighted) number of data-data, random-random and data-random pairs respectively in a narrow bin of separation r . The subscripts 1 and 2 again correspond to the two surveys. The two random catalogues were generated within the joint sur-

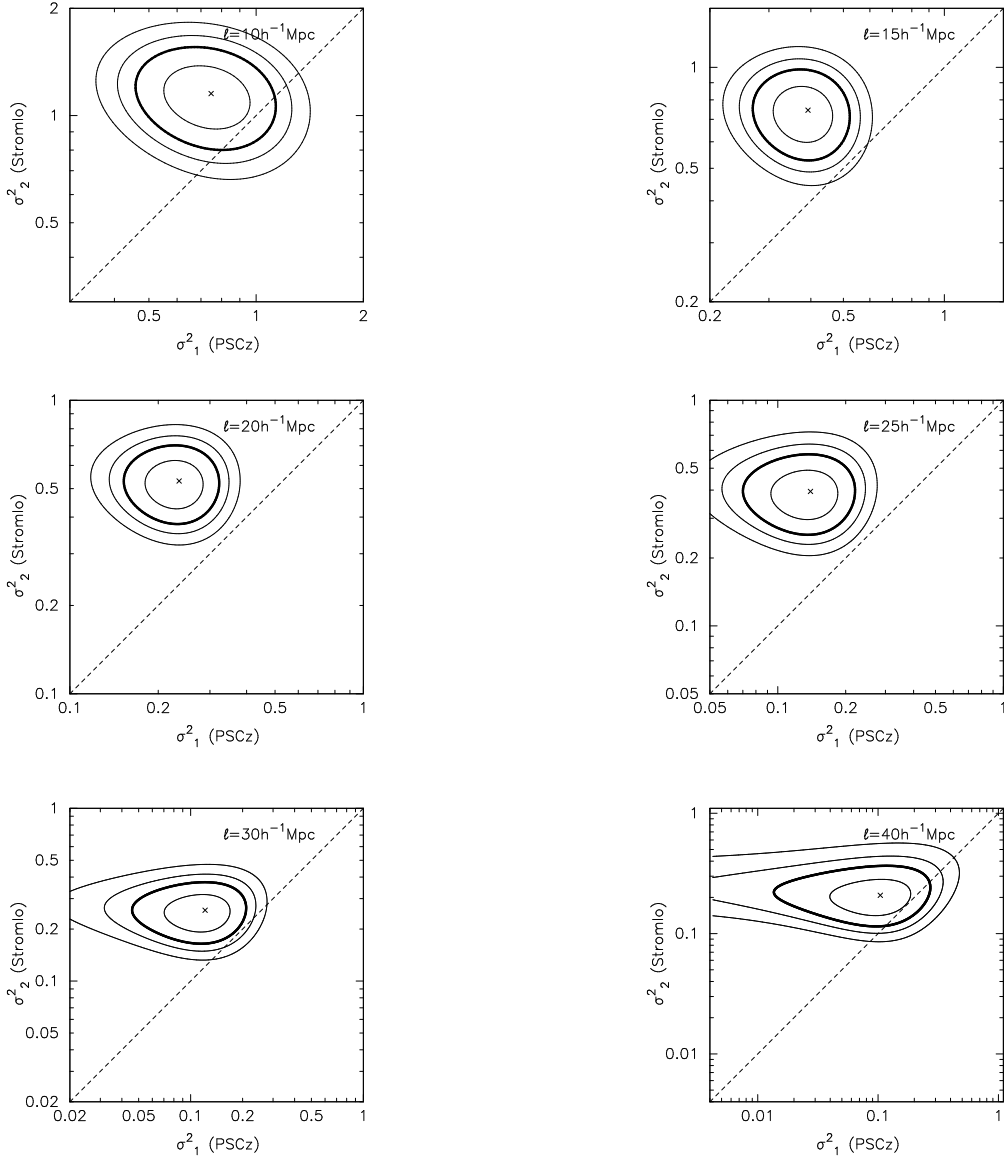


Figure 6: Contour maps of the likelihood of variances of PSCz and Stromlo galaxy counts for a range of cell sizes. In each case we have assumed $\sigma_{12}^2 = \sigma_1\sigma_2$. The contours show where $2 \ln(\mathcal{L}/\mathcal{L}_{\max})$ is equal to 2.28, 5.99, 9.21 and 13.81. These correspond to 68%, 95% (thick contour), 99% and 99.9% confidence intervals respectively, according to a chi-squared distribution with two degrees of freedom. The dotted line shows $\sigma_1^2 = \sigma_2^2$

Table 1: Relative bias as a function of cell size.

ℓ	$b_{\text{rel}}(95\%)$
10	1.24 (0.97–1.59)
15	1.38 (1.15–1.68)
20	1.50 (1.25–1.86)
25	1.68 (1.31–2.34)
30	1.46 (1.12–2.30)
40	1.42 (0.96–3.30)

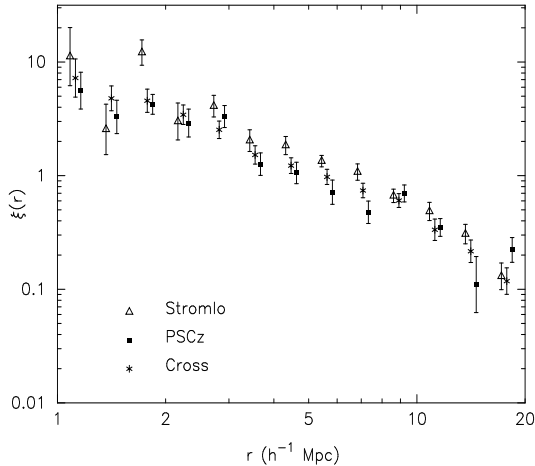


Figure 7: The Stromlo, PSCz and cross-correlation functions for the overlapping volume. The 1σ error bars were generated using the 27 pairs of mock catalogues.

vey volume, each with the correct corresponding radial selection function. The selection functions were determined by integrating the published luminosity functions for the two surveys. For Stromlo-APM we use a Schechter function with input parameters $\alpha = -0.97$, $M^* = -19.50$ and $\phi^* = 1.4 \times 10^{-2} h^3 \text{Mpc}^{-3}$ (Loveday et al. 1992). For the *IRAS* luminosity function we use the parametric form

$$\phi(L) = C \left(\frac{L}{L^*} \right)^{(1-\alpha)} \exp \left[-\frac{1}{2\sigma^2} \log_{10}^2 \left(1 + \frac{L}{L^*} \right) \right] \quad (20)$$

with $C = 2.6 h^3 \text{Mpc}^{-3}$, $\alpha = 1.09$, $\sigma = 0.724$ and $L^* = 10^{8.47} h^{-2} L_{\odot}$ (Saunders et al. 1990). Each random catalogue contains 2×10^4 data points.

To each galaxy or random in a pair we assign the weight

$$w_i = \frac{1}{1 + 4\pi n(r_i) J_3(r)}, \quad J_3(r) = \int_0^r \xi(x) dx, \quad (21)$$

where r_i is the radial distance to the galaxy. This weighting scheme can be shown to give the minimum uncertainty in $\xi(r)$ on scales where $\xi(r) \lesssim 1$. We determine the input quantity J_3 using determinations of the *IRAS* and Stromlo correlation functions by previous authors. We use power law fits of the form $\xi(r) = (r/r_0)^{-\gamma}$. Fisher et al. (1994) have measured the correlation function of the *IRAS* 1.2-Jy survey and find that their results are well described by a power law with $r_0 = 4.53 h^{-1} \text{Mpc}$ and $\gamma = 1.28$. The Stromlo-APM correlation function has been determined by Loveday et al. (1995) and they obtain a power law with $r_0 = 5.9 h^{-1} \text{Mpc}$ and $\gamma = 1.47$. The 1σ error bars were calculated using the 27 pairs of mock PSCz and Stromlo catalogues under the same weighting scheme.

The three correlation functions are shown in figure 7. The Stromlo correlation function is in general greater

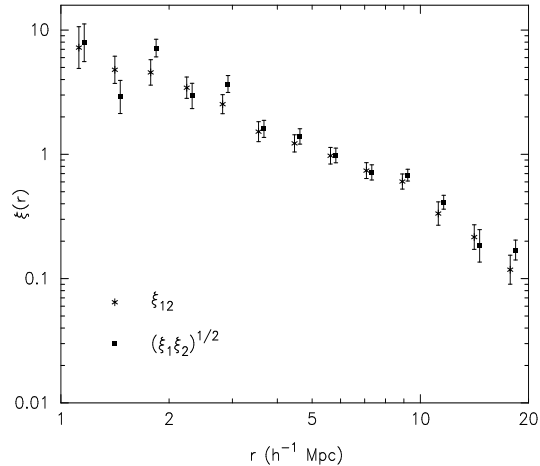


Figure 8: The cross correlation function, ξ_{12} , for PSCz and Stromlo-APM and the quantity $(\xi_1 \xi_2)^{1/2}$ where ξ_1 and ξ_2 are the individual two point correlation functions. The error bars show one standard deviations calculated from the mock catalogues.

than that of PSCz, consistent with the cell count variances. As expected, the cross correlation function lies between the two individual functions.

The cross-correlation function ξ_{12} and the quantity $(\xi_1 \xi_2)^{1/2}$ are shown in Figure 8. This shows that these two quantities are consistent within their error bars, i.e. in good agreement with the linear biasing hypothesis. If the galaxy distributions were related in some other way - for example non-linear or stochastic biasing - we would expect ξ_{12} to lie below $(\xi_1 \xi_2)^{1/2}$. We see from Figure 8 that there is no such systematic difference. Whereas the counts in cells technique was only used to investigate structure on scales of $\ell \geq 10 h^{-1} \text{Mpc}$, here we see that the linear bias model is consistent right down to scales of $\sim 1.5 h^{-1} \text{Mpc}$. On scales smaller than this our determination of the three correlation functions becomes highly uncertain as there are a low number of galaxy pairs at these separations.

The relative bias $b_{\text{rel}} \equiv b_{\text{Stromlo}}/b_{\text{PSCz}}$ is estimated from the correlation functions at distances in the range $1 - 20 h^{-1} \text{Mpc}$ using

$$b_{\text{rel}} = \left(\frac{\xi_{\text{Stromlo}}}{\xi_{\text{PSCz}}} \right)^{1/2} \quad (22)$$

and is plotted in Figure 9. Beyond separations of $r \approx 30 h^{-1} \text{Mpc}$ the relative bias becomes highly uncertain as both correlation functions are consistent with zero on these scales. Where the 1σ error bars are not too large, we see that the relative bias remains roughly constant over the separation range $r < 20 h^{-1} \text{Mpc}$ and has a mean value of $b_{\text{rel}} = 1.29 \pm 0.07$, where the error is estimated from the mock catalogues. A calculation of $\chi^2 = \sum_{i=1}^N (b_i - \bar{b})^2 / \sigma_i^2$ gives a reduced chi-squared of 1.76. Although a little high, this value does not rule out

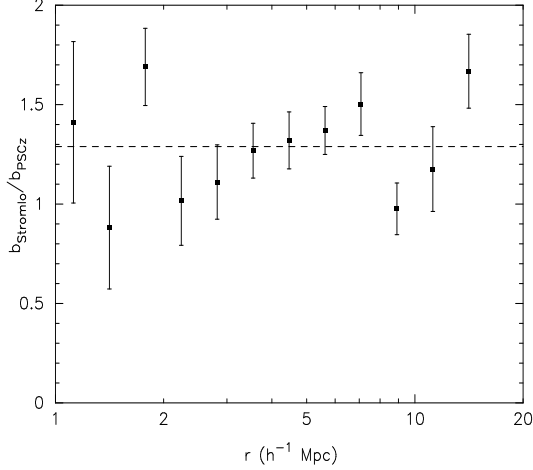


Figure 9: The relative bias between the Stromlo and PSCz correlation functions over the range $1 - 20 h^{-1}\text{Mpc}$. The dotted line is the mean value $b_{\text{Stromlo}}/b_{\text{PSCz}} = 1.29$

the hypothesis that the relative bias is unchanging with scale within a 95% confidence limit. (Note that caution should be taken in the interpretation of this χ^2 value since the measurements of the values of b on different scales are not independent.) More importantly, we note that there is no obvious trend in the relative bias with scale.

We estimate the average correlation coefficient $R = \xi_{12}/\sqrt{\xi_1\xi_2}$ by taking an unweighted mean over data points in the range $2 h^{-1}\text{Mpc} < r < 20 h^{-1}\text{Mpc}$; the result is $R = 0.93 \pm 0.06$, where we again derive the 1σ error from the simulations. This can be used to place limits on “stochastic bias” as discussed later.

5 THE TEGMARK ‘NULL-BUSTER’ TEST

Tegmark and Bromley (1998) use a generalised χ^2 -statistic to directly compare cell counts of different galaxy populations in the Las Campanas Redshift Survey. We have applied their method to compare the clustering in PSCz and Stromlo-APM. We bin the galaxies from the two surveys using the cells described earlier and, for each of N_c cells, we calculate the overdensities $g_i^{(\text{PSCz})} = N_i^{(\text{PSCz})}/\langle N \rangle^{(\text{PSCz})} - 1$ and $g_i^{(\text{Stromlo})} = N_i^{(\text{Stromlo})}/\langle N \rangle_i^{(\text{Stromlo})} - 1$ ($i = 1, \dots, N_c$). The expected counts $\langle N \rangle_i^{(\text{PSCz})}$ and $\langle N \rangle_i^{(\text{Stromlo})}$ were calculated using the respective selection functions and the joint survey mask. If the galaxy densities are related by linear bias, then there will exist a value for b_{rel} such that the (column) vector

$$\Delta g = g_{\text{Stromlo}} - b_{\text{rel}} g_{\text{PSCz}} \quad (23)$$

is consistent with shot noise. The covariance matrix of Δg is diagonal and (for density fluctuations $\lesssim 1$) is given by

$$\mathbf{N} \equiv \frac{1}{\langle N \rangle_{\text{Stromlo}}} + \frac{b_{\text{rel}}^2}{\langle N \rangle_{\text{PSCz}}} \quad (24)$$

Our null hypothesis is that, for a given value of b , $\langle \Delta g \rangle = 0$ and $\langle \Delta g \Delta g^t \rangle = \mathbf{N}$. We might choose to test this hypothesis by calculating the statistic $\chi^2 = \Delta g^t \mathbf{N}^{-1} \Delta g$. The number of “sigmas” at which the null hypothesis is ruled out is then $\nu = (\chi^2 - N_c)/\sqrt{2N_c}$. If we have an alternative hypothesis that there is an extra signal with covariance matrix \mathbf{S} , such that $\langle \Delta g \Delta g^t \rangle = \mathbf{N} + \mathbf{S}$, then Tegmark (1998) shows that the statistic $\Delta g^t \mathbf{N}^{-1} \mathbf{S} \mathbf{N}^{-1} \Delta g$ will provide a more sensitive test (by using our prior knowledge of the signal covariance matrix). The significance at which the null hypothesis can be ruled out is then given by

$$\nu \equiv \frac{\Delta g^t \mathbf{N}^{-1} \mathbf{S} \mathbf{N}^{-1} \Delta g - \text{tr} \mathbf{N}^{-1} \mathbf{S}}{[2 \text{tr} \{ \mathbf{N}^{-1} \mathbf{S} \mathbf{N}^{-1} \mathbf{S} \}]^{1/2}} \quad (25)$$

If the biasing is non-linear then the deviations from linearity would be correlated with large scale structure. We thus choose the matrix \mathbf{S} to be the covariance between cell overdensities calculated using the PSCz correlation function, i.e. the volume-average of $\xi(r_{ij})$ over cells i and j . (Note that ν depends only on the shape of \mathbf{S} , not its amplitude). The resulting values of ν as a function of b for a range of cell sizes are shown in Figure 10.

As expected we see that extreme values of the relative bias parameter are ruled out with high significance (i.e., the clustering in each individual survey is inconsistent with pure shot noise). The position of the minimum indicates the most likely value of b_{rel} : Table 2 shows this value for each cell size. The 1σ errors are estimated using the 27 simulated catalogues from § 2.1. For all cell sizes we see that the minimum value of ν is typically not much larger than 1, again suggesting that the two surveys are consistent with a linear relative bias. At all scales the relative bias is consistent with $b_{\text{rel}} \approx 1.3$, again above unity but slightly lower than the values estimated in §3.

6 CONCLUSIONS

We have compared the clustering of two redshift surveys (the new *IRAS*-selected PSCz survey, and the optically-selected Stromlo-APM survey) within their common region of space. Three complementary methods have been used: the counts-in-cells method, the two-point correlation function, and the Tegmark ‘null-buster’ test. In all three cases the results are consistent with a linear biasing model, i.e. $\delta_{\text{Stromlo}} = b_{\text{rel}} \delta_{\text{PSCz}}$ with $b_{\text{rel}} = b_{\text{Stromlo}}/b_{\text{PSCz}} \approx 1.3 \pm 0.1$. There is little evidence for variation of the relative bias over the range of scales from $\sim 5 - 30 h^{-1}\text{Mpc}$. We find a lower

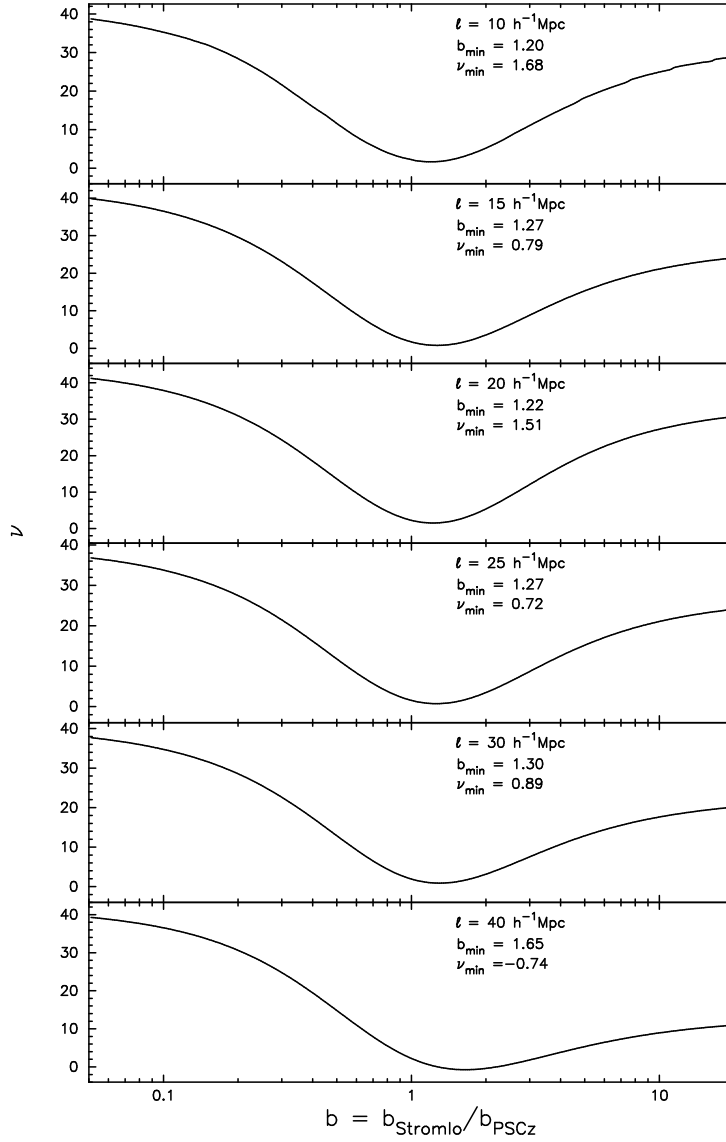


Figure 10: The function $\nu(b_{\text{rel}})$, i.e. number of “sigmas” at which the linear bias $g_{\text{Stromlo}} = b_{\text{rel}}g_{\text{PSCz}}$ can be ruled out as a function of b_{rel} . The position of the minimum is given for each cell size.

Table 2: Relative bias as a function of cell size.

ℓ	b_{rel}
15	1.27 ± 0.11
20	1.22 ± 0.09
25	1.27 ± 0.12
30	1.30 ± 0.16
40	1.65 ± 0.13

limit on the correlation coefficient $R \gtrsim 0.85$ on scales $\sim 10 - 20 h^{-1}\text{Mpc}$.

Our value for the relative bias is in quite good agreement with earlier estimates; Baker *et al.* (1998) found $b_{\text{rel}} = 1.4$; Willmer *et al.* found $b_{\text{rel}} = 1.20 \pm 0.07$ and Saunders *et al.* (1992) obtained a value of $b_{\text{rel}} = 1.38 \pm 0.12$ in real space. Our high value for R seems somewhat unexpected in view of the results of Tegmark & Bromley (1998), who found values of R as low as 0.5 comparing various pairs of spectral classes in the Las Campanas redshift survey. However, their results are not directly comparable with ours for several reasons: firstly, they used considerably smaller cells of size $\sim 6 h^{-1}\text{Mpc}$, and secondly our galaxy classes (PSCz and Stromlo) do not correspond closely to the classes used by TB; Stromlo contains a mix of early and late type galaxies, while PSCz is weighted towards late-type spirals with a preference for high surface brightnesses (hence higher dust temperatures) and merging systems.

We may translate a lower limit on R into an upper limit on ‘stochastic’ bias if it is independent between the two galaxy classes, as follows: using the notation of Dekel & Lahav (1998), we may define the stochasticity $\epsilon_i (i = 1, 2)$ by $g_i = \langle g_i | \delta \rangle + \epsilon_i$ where the angle brackets denote averages over δ . Then

$$\begin{aligned} \text{Cov}(g_1, g_2) &= \langle \langle g_1 | \delta \rangle \langle g_2 | \delta \rangle \rangle + \langle \epsilon_1 \epsilon_2 \rangle \\ &\equiv \sigma^2 (\tilde{b}_{12}^2 + \sigma_{b12}^2) \quad \text{thus} \end{aligned} \quad (26)$$

$$\begin{aligned} R &\equiv \text{Cov}(g_1, g_2) / \sigma_{g1} \sigma_{g2} \\ &= \frac{\tilde{b}_{12}^2 + \sigma_{b12}^2}{\left[(\tilde{b}_1^2 + \sigma_{b1}^2)(\tilde{b}_2^2 + \sigma_{b2}^2) \right]^{1/2}} \end{aligned} \quad (27)$$

where the first line follows since the cross terms $\langle \langle g_1 | \delta \rangle \epsilon_2 \rangle$ vanish, and the second line follows from the definitions of \tilde{b}_{12} and σ_{b12} , analogous to the definitions $\tilde{b}_1^2 \equiv \langle \langle g_1 | \delta \rangle^2 \rangle / \sigma^2$ and $\sigma_{b1}^2 \equiv \langle \epsilon_1^2 \rangle / \sigma^2$ in DL, and σ^2 is the mass variance on a given smoothing scale. From numerical studies, DL find that $\tilde{b}/\hat{b} \sim 1 - 1.15$, so it is probably reasonable to assume $\tilde{b}_{12} \approx (\tilde{b}_1 \tilde{b}_2)^{1/2}$. Then if we assume $\sigma_{b12} = 0$ (i.e. assuming that the ‘stochastic’ bias is independent between surveys), and adopting $\tilde{b}_{\text{PSCz}} = 1$, $\tilde{b}_{\text{Stromlo}} = 1.3$, we find that $R \geq 0.8$ would imply $\sigma_{b1}^2 < 0.56$ and $\sigma_{b2}^2 < 0.95$, Likewise $R \geq 0.9$ would imply $\sigma_{b1}^2 < 0.23$ and $\sigma_{b2}^2 < 0.39$. DL show that $b_{\text{var}}^2 = \tilde{b}^2 + \sigma_b^2$, so the ‘fractional stochasticity’ is effectively σ_b^2 / \tilde{b}^2 , i.e. the ratio of stochastic variance to deterministic variance in galaxy density. If the fractional stochasticity is equal for the two surveys, such that $\sigma_{b1}^2 / \tilde{b}_1^2 = \sigma_{b2}^2 / \tilde{b}_2^2 = y$, then the above assumptions lead to $1 + y = R^{-1}$. Clearly, these numbers are illustrative rather than definitive: the assumption $\sigma_{b12}^2 = 0$ may not be satisfied in practice since there could be a ‘second parameter’ in addition to the mass overdensity e.g. local shear, gas temperature etc. which affects the formation of both *IRAS* and optical galaxies. But this argument does suggest that ‘stochastic’ bias which

preferentially affects either the earliest or latest type galaxies is unlikely to be severe.

Our results are encouraging for velocity field studies, in that that they suggest that large-scale density fields (usually estimated from *IRAS* galaxies) should also be a good match to those which would be estimated from all-sky optical surveys (currently rather limited in extent); this supports the conclusions of Baker *et al.* (1998).

In a future paper we plan to apply the tests considered here to the PSCz and the Optical Redshift Survey (Santiago *et al.* 1995), which gives a higher sampling density than Stromlo-APM and thus may provide stronger constraints.

ACKNOWLEDGEMENTS

We are very grateful to many observers, especially Marc Davis, Tony Fairall, Karl Fisher & John Huchra for supplying redshifts in advance of publication. We thank the staff at the INT, AAT and CTIO telescopes for support, especially Hernan Tirado and Patricio Ugarte at CTIO. MDS is supported by a PPARC studentship, W. Sutherland is supported by a PPARC Advanced Fellowship, and W. Saunders is supported by a Royal Society Fellowship. GE thanks PPARC for the award of a Senior Fellowship.

REFERENCES

- Baker, J.E., Davis, M., Strauss, M.A., Lahav, O., Santiago, B., 1998, ApJ, in press (astro-ph/9802173)
- Branchini, E. *et al.*, 1999, MNRAS, in press
- Canavezes, A. *et al.*, 1998, MNRAS, 297, 777
- Coles, P., 1993, MNRAS, 262, 1065
- De Souza R.E., Capelato V., Arakaki L., Logullo C., 1982, ApJ, 263, 557
- Dekel, A., Lahav, O., 1998, ApJ, in press (astro-ph/9806193)
- Dressler, A., 1980, ApJ, 236, 351
- Efstathiou, G., Kaiser, N., Saunders, W., Lawrence, A., Rowan-Robinson, M., Ellis, R.S., Frenk, C.S., 1990, MNRAS, 247, 10P
- Efstathiou G., 1995, MNRAS, 276, 1425 (E95)
- Fisher, K.B., Davis, M., Strauss, M., Yahil, A., Huchra, J., 1994, MNRAS, 266, 50
- Guzzo, L., Strauss, M.A., Fisher, K.B., Giovanelli, R., Haynes, M.P., 1997, ApJ, 489, 37
- Hamilton, A.J.S., 1993, ApJ, 417, 19
- Hubble, E.P., 1936, ‘The Realm of the Nebulae’, Oxford Univ. Press.
- Hubble E., Humason M.L., 1931, ApJ, 74, 43
- Jing, Y.P., 1998, astro-ph/9805202
- Kaiser, N., 1984, ApJ, 284, L9
- Lahav, O., Nemiroff, R.J., Piran, T., 1990, ApJ, 350, 11
- Loveday, J., Efstathiou, G., Peterson, B.A., Maddox, S.J., 1992, ApJ, 400, L43
- Loveday, J., Peterson, B.A., Maddox, S.J., Efstathiou, G., 1996, ApJ Supp, 107, 201
- Maddox, S.J., Sutherland, W.J., Efstathiou, G., Loveday, J., 1990, MNRAS, 243, 692
- Mann, R.G., Saunders, W., Taylor, A.N., 1996, MNRAS, 279, 636

- Mann, R.G., Peacock, J.A., Heavens, A.F., 1998, MNRAS, 293, 209
- Mo H.J., Jing Y.P. & Börner G., 1992, ApJ, 392, 452
- Mo, H.J., White, S.D.M., 1996, MNRAS, 282, 347
- Narayanan, V.K., Berlind, A.A., Weinberg., D.H., 1998, astro-ph/9812002
- Oemler A., 1974, ApJ, 194, 1
- Oliver, S. *et al.*, 1996, MNRAS, 280, 673
- Pen, U.L., 1998, ApJ, 504, 601
- Postman M., Geller M.J., 1984, ApJ, 281, 95
- Rowan-Robinson M., Lawrence A., Saunders W., Crawford J., Ellis R., Frenk C.S., Parry I., Xiaoyang X., Allington-Smith J., Efstathiou G., Kaiser N., 1990, MNRAS, 247, 1
- Rowan-Robinson M., Saunders, W., Lawrence A., Leech, K., 1992, MNRAS, 253, 485
- Saunders, W., Rowan-Robinson, M., Lawrence, A., 1992, MNRAS, 258, 134
- Saunders, W. *et al.*, 1997, in "Wide-Field Spectroscopy and the Distant Universe", eds. S. Maddox and A. Aragon-Salamanca, World Scientific Press, Singapore
- Santiago, B.X., Strauss, M.A., Lahav, O., Davis, M., Dressler, A., Huchra, J.P., 1995, ApJ, 446, 457
- Saunders, W., Rowan-Robinson, M., Lawrence, A., Efstathiou, G., Kaiser, N., Ellis, R.S., Frenk, C.S., 1990, MNRAS, 242, 318
- Scherrer, R., Weinberg, D., 1998, ApJ, 504, 607
- Shectman, S.A., Landy, S.D., Oemler, A., Tucker, D.L., Lin, H., Kirshner, R.P., Schechter, P.L., 1996, ApJ, 470, 172
- Sutherland, W. *et al.*, 1999, MNRAS, in press
- Tegmark, M., 1998, astro-ph/9809001
- Tegmark, M., Bromley, M., 1998, astro-ph/9809324
- Vogeley, M.S., Park, C., Geller, M.J., Huchra, J.P., 1992, ApJ, 391, L5
- Whitmore B.C., Gilmore D.M., Jones C., 1993, ApJ, 407, 489